5-27-2005

Ab initio calculation of bowl, cage, and ring isomers of C_{20} and C_{20}^-

Wei An
University of Nebraska-Lincoln

Yi Gao
University of Nebraska-Lincoln, ygao3@Unl.edu

Satya S. Bulusu
University of Nebraska-Lincoln, sbulusu@iiti.ac.in

Xiao Cheng Zeng
University of Nebraska-Lincoln, xzeng1@unl.edu

Ab initio calculation of bowl, cage, and ring isomers of C_{20} and C_{20}^-

Wei An, Yi Gao, Satya Bulusu, and X. C. Zeng[a)]
Department of Chemistry, University of Nebraska-Lincoln, Lincoln, Nebraska 68588

(Received 7 February 2005; accepted 16 March 2005; published online 27 May 2005)

High-level *ab initio* calculations have been carried out to reexamine relative stability of bowl, cage, and ring isomers of C_{20} and C_{20}^-. The total electronic energies of the three isomers show different energy orderings, strongly depending on the hybrid functionals selected. It is found that among three popular hybrid density-functional (DF) methods B3LYP, B3PW91, PBE1PBE, and a new hybrid-meta-DF method TPSSKCIS, only the PBE1PBE method (with cc-pVTZ basis set) gives qualitatively correct energy ordering as that predicted from *ab initio* CCSD(T)/cc-pVDZ [CCSD(T)—coupled-cluster method including singles, doubles, and noniterative perturbative triples; cc-pVDZ—correlation consistent polarized valence double zeta] as well as from MP4(SDQ)/cc-pVTZ [MP4—fourth-order Moller–Plesset; cc-pVTZ—correlation consistent polarized valence triple zeta] calculations. Both CCSD(T) and MP4 calculations indicate that the bowl is most likely the global minimum of neutral C_{20} isomers, followed by the fullerene cage and ring. For the anionic counterparts, the PBE1PBE calculation also agrees with MP4/cc-pVTZ calculation, both predicting that the bowl is still the lowest-energy structure of C_{20}^- at $T=0$ K, followed by the ring and the cage. In contrast, both B3LYP/cc-pVTZ and B3PW91/cc-pVTZ calculations predict that the ring is the lowest-energy structure of C_{20}^-. Apparently, this good reliability in predicting the energy ordering renders the hybrid PBE method a leading choice for predicting relative stability among large-sized carbon clusters and other carbon nanostructures (e.g., finite-size carbon nanotubes, nano-onions, or nanohorns). The relative stabilities derived from total energy with Gibbs free-energy corrections demonstrate a changing ordering in which ring becomes more favorable for both C_{20} and C_{20}^- at high temperatures. Finally, photoelectron spectra (PES) for the anionic C_{20}^- isomers have been computed. With binding energies up to 7 eV, the simulated PES show ample spectral features to distinguish the three competitive C_{20}^- isomers. © *2005 American Institute of Physics*. [DOI: 10.1063/1.1903946]

I. INTRODUCTION

Over the past decade considerable attention has been paid in searching for the ground-state C_{20} isomer from either *ab initio* calculations[1–17] or experimental measurements.[18–22] The studies can be traced back to the discovery[23] of the fullerene structure of C_{60}, and, thereafter, of their novel properties such as high temperature superconductivity.[24–26] Besides the best known "bucky ball" C_{60}, a wide range of fullerenes with "magic numbers" has been predicted theoretically and observed experimentally.[22,27–29] Fullerenes are graphitic hollow-cage structures incorporating exactly 12 pentagons without restriction of the number of hexagon. Among the fullerene cages, C_{60} has the icosahedral cage structure with each pentagons surrounded by five hexagons and is therefore highly aromatic and remarkably stable; in contrast, C_{20} fullerene cage (see Fig. 1) consists of solely 12 pentagonal rings that form a dodecahedron with no hexagons incorporated, resulting in an extreme curvature. C_{20} cage is therefore the smallest and the most strained fullerene structure. It has been predicted that the solid form of C_{20} fullerene is a promising candidate for high-temperature superconductor due to its larger electron-phonon coupling than C_{60} fullerene.[30] C_{20} cluster family has two other distinctive low-lying members,[1,22] namely, the monocyclic ring and corannulenelike bowl isomers. The bowl isomer is an open structure that has one central graphitic pentagon surrounded by five hexagonal rings. In fact, the bowl could be considered as a piece of fragment of C_{60} fullerene. These three geometrically very different C_{20} isomers are close in energy and could be potentially used as building blocks to the C_{60} fullerene formation.[29,31,32] Prinzbach *et al.*[22] have recently reported the gas-phase production and photoelectron spectroscopy characterizations of cage and bowl isomers of C_{20}. With respect to how fullerenes are formed from small carbon fragments, two growth mechanisms have been proposed–the "fullerene road" and the "pentagon road."[33] In the fullerene road, rings generated from small carbon fragments isomerize into fullerenes; in contrast, bowls, as the starting point of the pentagon road, grow to cup and to fullerenes by adding two carbon atoms at a time. All these advances have motivated more and more research interests in C_{20} clusters and called for *ab initio* theoretical calculations at higher levels to provide more accurate molecular and other relevant chemical properties for large fullerenes.

However, it has been more than a decade that the issue of relative stability of C_{20} isomers remains controversial. A variety of theoretical and experimental approaches have been attempted to explore the structure characterizations and rela-

[a)]Electronic mail: xczeng@phase2.unl.edu

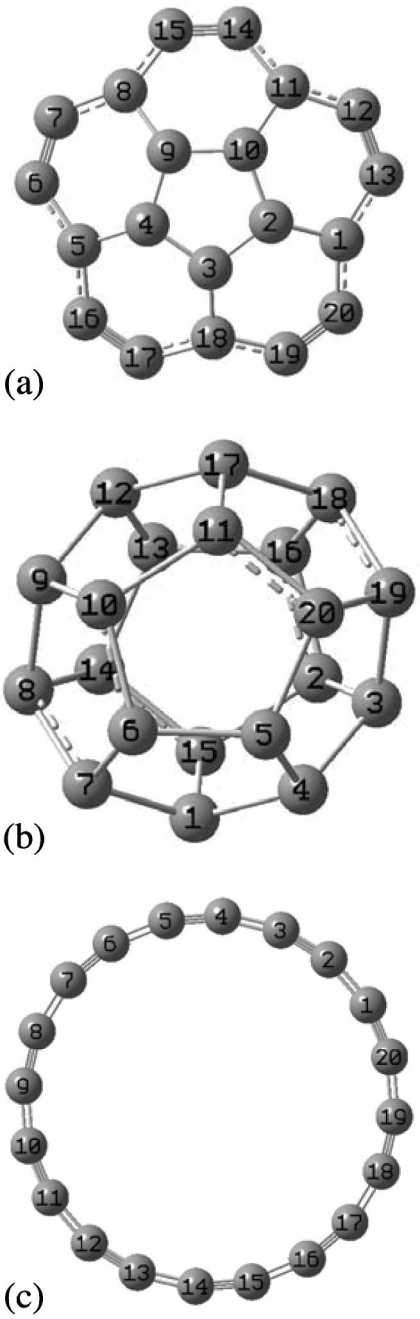

FIG. 1. Structure of the three C_{20} isomers optimized at MP2/cc-pVDZ level. (a) Bowl (D_{5v}). (b) Cage (D_{3d}). (c) Ring (D_{10h}).

tive stability of the three C_{20} isomers. Because of high reactivity of C_{20} isomers, the difficulties in performing experiments undoubtedly exist. Most experimental measurements[18–22] have demonstrated that the ring isomer of C_{20} is the most stable structure because the ring is the dominant species generated in graphite laser vaporization sources and first observed among other structures of C_{20}. *Ab initio* calculations thus far have given different energy orderings of C_{20} isomers, strongly depending on the theoretical methods selected. One complication is that all experimental results have been derived from C_{20}^- or C_{20}^+ cluster ions at high temperature, whereas *ab initio* calculations have been mostly performed for C_{20} neutral isomers at $T=0$ K. Thus, the total energy given by *ab initio* calculations cannot be directly compared with the experiments which typically generate the most stable C_{20} isomer at high temperatures.[1–17] Brabec *et al.*[32] applied quantum molecular-dynamics simulations with Car–Parrinello method and showed that the free energy of C_{20} clusters favors a transformation from a closed cage structure at low temperatures to a more open corrannulenelike bowl structure and ultimately to a ring structure at high temperatures. Castro *et al.*[10] calculated the optical response of C_{20} isomers by using time-dependent density-functional theory to characterize their geometry and to identify the ground state. Romero *et al.*[11] proposed to use NMR shifts as a way to distinguish the structure of C_{20} isomers although a question has been raised that whether the NMR technique is applicable in the rarefied environment of C_{20} isomers. Quantum Monte Carlo (QMC) calculations[7–9] have predicted that the bowl structure is the global minimum, followed by the ring and cage. Nevertheless, high-resolution ion-mobility measurements,[18,19] the surface phasmon polariton Raman spectra,[20] and ultraviolet photoelectron spectra[21] all indicate that neither the bowl nor the cage structures of C_{20} can even be observed under the experimental conditions.

Numerous *ab initio* molecular-orbital and density-functional theory (DFT) calculations for C_{20} isomers have been reported in the last decade. Most calculations used relatively lower levels of theory or smaller basis sets. Results have been tabulated by several researchers.[2–4,7] The disparities in the relative stability of bowl, cage, and ring isomers of C_{20} were first reported by Raghavachari *et al.* The Hartree–Fock (HF) level of theory with the 6-31G(d) (Ref. 34) basis set **(**double split for the valence basis functions, contracted $[3s2p]$ plus polarization set $(1d)$**)** predicts the ring structure is the most stable, followed by the bowl (1.35 eV higher in energy) and cage (4.03 eV higher). However, DFT (Ref. 35) calculations with local density approximation (LDA) and the 6-311G(d) basis set **(**triple split for the valence basis functions, contracted $[4s3p]$ plus polarization set $(1d)$**)** totally reverse the ordering, which predicts that the cage is the most stable, followed by the bowl (+1.01 eV) and ring (+3.84 eV). The energy ordering can be reversed back to the HF ordering when generalized-gradient approximation corrections are employed, with which the energy difference again depends on the correction functional used.

With the computer speed greatly enhanced over the past few years, high-level *ab initio* calculations have become feasible for medium-sized molecules. In this paper, we present DFT calculations with a large basis set as well as high-level *ab initio* molecular orbital calculations with modest to large basis sets for the bowl, cage and ring isomers of C_{20} and C_{20}^-. The objective is to reexamine their relative stability and to simulate their photoelectron spectra with the ultimate goal of having a definite assignment of energy ordering for the C_{20} and C_{20}^- isomers.

II. COMPUTATIONAL DETAILS

All calculations were performed using GAUSSIAN03, Revision B.03 package.[36] First, geometry optimizations and frequency calculations were performed respectively using DFT methods with three popular hybrid exchange-correlation

TABLE I. Computed geometries (angstroms, degrees) and symmetries for neutral C_{20} isomers.

Structure	B3LYP/ cc-pVTZ[a]	B3PW91/ cc-pVTZ[a]	PBE1PBE/ cc-pVTZ[a]	TPSSKCIS /cc-pVTZ[a]	MP2/ cc-pVDZ[b]	LDA[c]	PBE[c]	MP2/ TZV2d1f[d]
Ring	D_{10h}	D_{10h}	D_{10h}	D_{10h}	D_{10h}	D_{10h}	D_{10h}	D_{10h}
C1–C20	1.226	1.227	1.225	1.241	1.267	1.244	1.241	1.251
C1–C2	1.341	1.340	1.341	1.334	1.352	1.334	1.336	1.337
θ(C2–C1–C20)	162.0	162.0	162.0	162.0	162.0	N/A	N/A	N/A
Bowl	C_{5v}	C_{5v}	C_{5v}	C_{5v}	C_{5v}	C_{5v}	C_{5v}	C_{5v}
C2–C10	1.424	1.422	1.420	1.426	1.435	1.423	1.425	1.423
C10–C11	1.424	1.423	1.421	1.436	1.444	1.434	1.435	1.434
C11–C12	1.414	1.410	1.409	1.414	1.424	1.410	1.414	1.411
C12–C13	1.238	1.239	1.237	1.250	1.286	1.249	1.246	1.269
θ(C1–C2–C10)	123.7	123.8	123.9	123.8	123.8	N/A	N/A	N/A
θ(C10–C11–C12)	107.1	106.9	106.8	106.8	107.5	N/A	N/A	N/A
Cage	D_{3d}	D_{3d}	D_{3d}	D_{3d}	D_{3d}	D_{3d}	D_{3d}	D_{3d}
C1–C4	1.439	1.435	1.433	1.434	1.456	1.443	1.443	1.446
C5–C6	1.445	1.442	1.440	1.449	1.463	1.450	1.450	1.484
C10–C11	1.514	1.508	1.506	1.515	1.516	1.510	1.510	1.510
C6–C10	1.400	1.397	1.395	1.406	1.432	1.409	1.407	1.429

[a]Symmetry obtained within a tolerance of 0.05 Å.
[b]Symmetry obtained within a tolerance of 0.001 Å.
[c]Reference 13.
[d]Reference 16.

functionals, namely, B3LYP,[37,38] B3PW91,[39,40] and PBE1PBE,[41,42] and a newly developed hybrid meta functional, TPSSKCIS.[43] A large cc-pVTZ basis set[44] **(**Dunning's correlation consistent polarized valence triple zeta, contracted [4*s*3*p*] plus polarization set (2*d*1*f*)**)** was chosen in these DFT calculations. To assess the effect on isomer structures due to different levels of theory, we also run geometry optimization by using the second-order Moller–Plesset perturbation theory[45–47] (MP2) (Refs. 48–50) with a modest cc-pVDZ basis set **(**correlation consistent polarized valence double zeta, contracted [3*s*2*p*] plus polarization set (1*d*)**)**. Unless specified, all calculations at the DFT and MP2 level were performed at the corresponding DFT and MP2 optimized geometries. In particular, the harmonic vibrational frequency analyses were carried out to assure that the final optimized structures give no imaginary frequencies. Next, based on the optimized geometries, single-point energy calculations were further computed using coupled-cluster method[51] at the level of CCSD(T) (Ref. 52) (including singles, doubles, and noniterative perturbative triples) with a modest basis set (cc-pVDZ). Finally, the fourth-order Moller–Plesset perturbation theory (MP4) (Refs. 53–55) with a large basis set [correlation consistent polarized valence triple zeta (cc-pVTZ)] was also used to calculate the single-point energies of neutral structures optimized at the MP2 level, and anionic structures at the PBE1PBE level of theory. Note that the number of basis functions (N) in the cc-pVTZ basis set for C_{20} isomers has been found to be 600. Considering resource usage scales roughly with multiple powers of N for MP2 (N^5) and CCSD(T) (N^7), much larger basis sets such as cc-pVQZ are impractical under the present computer technology.

III. RESULTS AND DISCUSSION

A. Optimized geometrical structure and vibrational frequencies

Small variations in bond lengths, angles, and dihedral angles within a cluster can lead to symmetry change and produce differences in its energy and related properties. It has been reported[2,4,9] that the energy ordering of bowl, cage, and ring isomers of C_{20} can be sensitive to the geometries obtained using different methods even if an identical method is used for single-point energy calculation. We have therefore examined five geometries optimized at the DFT and MP2 levels of theory and their differences on the relative stability of C_{20} isomers. Harmonic vibrational frequency analyses with the DFTs show no imaginary frequencies for the three isomers of C_{20}. Table I gives optimized geometries and symmetries of neutral C_{20} isomers obtained from the DFTs and MP2 calculations. All optimized geometrical structures show that the symmetry of bowl, cage, and ring is C_{5v}, D_{3d} and D_{10h}, respectively. It has long been known[1,3,4] that bowl has C_{5v} symmetry, cage has C_i or C_{2h} or C_2 symmetry, and ring has C_{10h} symmetry. However recent theoretical studies have shown that cage and ring might have higher symmetry (see Table I).[13,16,17] The highest possible symmetry of C_{20} isomers is I_h, with which the ground state is electronically degenerate. Due to the Jahn–Teller distorsion,[56] the I_h symmetry of C_{20} isomer is reduced to lower symmetry, thereby lowering the ground-state energy and giving a nonzero HOMO-LUMO (HOMO–highest occupied molecular orbital, LUMO—lowest unoccupied molecular orbital) gap. The ring shows two different alternating interatomic distances due to a second-order Jahn–Teller effect even though it has the highest symmetry (D_{10h}) among the three isomers. From Table I, the bond lengths and angles calculated with B3LYP,

TABLE II. Computed geometries (angstroms, degrees) and symmetries for anionic C_{20}^- isomers.

Structure	B3LYP/cc-pVTZ[a]	B3PW91/cc-pVTZ[a]	PBE1PBE/cc-pVTZ[a]	LDA[b]	PBE[b]
Ring	D_{10h}	D_{10h}	D_{10h}	D_{10h}	D_{10h}
C1–C20	1.241	1.242	1.240	1.257	1.255
C1–C2	1.327	1.326	1.327	1.324	1.326
θ(C2–C1–C20)	162.0	162.0	162.0	N/A	N/A
Bowl	C_{5v}	C_{5v}	C_{5v}	C_{5v}	C_2
					1.431
C2–C10	1.424	1.421	1.420	1.428	1.428
C10–C11	1.417	1.415	1.413	1.419	1.413
C11–C12	1.421	1.417	1.416	1.426	1.419
C12–C13	1.258	1.258	1.257	1.270	1.273
					1.251
θ(C1–C2–C10)	123.9	124.0	124.0	N/A	N/A
θ(C10–C11–C12)	107.7	107.5	107.4	N/A	N/A
Cage	D_{3d}	D_{3d}	D_{3d}	C_{2h}	C_{2h}
C1–C4	1.434	1.429	1.427	1.40	1.40
C5–C6	1.464	1.458	1.454	1.41	1.41
C10–C11	1.503	1.509	1.493	1.42–1.52	1.42–1.52
C6–C10	1.399	1.400	1.402		
C7–C8	1.419	1.413	1.414		

[a]Symmetry obtained within a tolerance of 0.05 Å.
[b]Reference 13.

B3PW91, and PBE1PBE functionals are all consistent with one another within 0.008 Å and 0.3°. Geometries obtained from the MP2 calculation show more differences with those from the DFTs but the symmetries are the same. Note that the symmetries derived from MP2 geometries are within a tolerance of 0.001 Å, compared to that of 0.05 Å for DFT geometries (C_1 symmetry obtained with the 0.001 Å tolerance).[57] For comparison, optimized geometries of C_{20}^- anions are listed in Table II. It is evident that the symmetry of bowl, cage, and ring remains the same despite of small changes within bond lengths and angles for the anionic counterparts. Using GAUSSVIEW3.0 molecular view package,[58] the geometrical structures of bowl, cage, and ring are displayed in Fig. 1, where the bond types are merely determined by bond lengths. Single, one-and-half, double, and triple bonds have been identified in the three structures of C_{20} isomers. Resonance configurations are expected within all three C_{20} isomers for stability reason.

B. Relative stability

The calculated total energies (hartree) and relative energies (eV) of neutral C_{20} isomers using DFTs, MP2, MP4, and CCSD(T) methods are tabulated in Tables III(A) and III(B). Previous calculations using CCSD(T) method are also listed in Table III(B). The four DFT methods yield quite different energy orderings. Both the B3LYP/cc-pVTZ and TPSSKCIS/cc-pVTZ calculations give the ordering of ring-bowl-cage with ring being the lowest in energy, consistent with previous calculations using the same hybrid functional B3LYP or BLYP but with smaller basis sets.[1,5,9] In contrast, the B3PW91/cc-pVTZ calculation yields bowl-ring-cage ordering, which is in agreement with the QMC predictions[7–9] as well as the BPW91//HF calculation by Grossman *et al.*[9] The PBE1PBE/cc-pVTZ calculation also predicts the bowl as the most stable structure but reverses the ordering of ring and cage from B3PW91/cc-pVTZ calculation. Note that Galli *et al.*[13] previously reported that the ring isomer has the lowest energy by using a nonhybrid exchange-correlation functional PBE//PBE with the plane-wave basis. The disparities in the energy ordering predicted from these DFT calculations further affirm the importance in accurately accounting for electron correlation effects in the fullerene clusters.[9]

For non-DFT calculations, the energy ordering given by MP2/cc-pVDZ calculation is cage-bowl-ring, in agreement with the previous calculations of MP2//LDA and MP2//SCF by Taylor *et al.*[2] but in disagreement with that by Wang *et al.*[3] and Murphy *et al.*,[5] who find that bowl is the most stable isomer. Moreover, the relative stability predicted by the CCSD(T) calculations with the fully optimized geometries based on either DFTs or MP2 is all consistent with one another, yielding the bowl-cage-ring ordering. In other words, the energy orderings given by the relative CCSD(T) energies are much less sensitive to the small structural differences due to different levels of theory (i.e., in the DFT or MP2 geometries). We note that the energy ordering given by the PBE1PBE/cc-pVTZ calculation is identical to that given by CCSD(T) calculation for this particular case. The fact that the energy ordering given by MP2 level is different from the one by CCSD(T) level reenforces the necessity of using high-level *ab initio* molecular-orbital calculations to predict the correct energy ordering. To further illustrate this point, single-point energy for the two lowest-energy isomers, i.e., bowl and cage, calculated at the MP4(SQD)/cc-pVTZ//MP2/cc-pVDZ level, has also been given in Table III. The calculation provides another stronger evidence that the bowl is appreciably lower in energy (0.91 eV) than the cage. As a

TABLE III. Calculated total energies (hartree) and relative energies (eV) for three neutral C_{20} isomers. The bold face denotes the lowest-energy isomer.

Method	Bowl	Cage	Ring
(A)			
B3LYP/cc-pVTZ	−761.733 005 3	−761.663 399 0	**−761.766 100 1**
B3PW91/cc-pVTZ	**−761.418 514 6**	−761.392 374 9	−761.407 956 2
PBE1PBE/cc-pVTZ	**−760.840 013 1**	−760.831 937 6	−760.804 973 7
TPSSKCIS/cc-pVTZ	−761.943 273 7	−761.902 504 8	**−761.971 765 9**
MP2/cc-pVDZ	−759.317 017 1	**−759.340 388 1**	−759.231 591 2
MP4(SDQ)/cc-pVTZ//MP2/cc-pVDZ	**−759.853 334 8**	−759.819 865 9	···
CCSD(T)/cc-pVDZ//B3PW91/cc-pVTZ	**−759.414 170 6**	−759.404 579 2	−759.326 357 6
CCSD(T)/cc-pVDZ//PBE1PBE/cc-pVTZ	**−759.412 149 0**	−759.401 994 3	−759.326 745 6
CCSD(T)/cc-pVDZ//MP2/cc-pVDZ	**−759.431 714 7**	−759.418 168 3	−759.341 783 4
(B)			
B3LYP/cc-pVTZ	0.00	1.89	−0.90
B3PW91/cc-pVTZ	0.00	0.71	0.29
PBE1PBE/cc-pVTZ	0.00	0.22	0.95
TPSSKCIS/cc-pVTZ	0.00	1.11	−0.78
MP2/cc-pVDZ	0.00	−0.64	2.32
MP4(SDQ)/cc-pVTZ//MP2/cc-pVDZ	0.00	0.91	···
CCSD(T)/cc-pVDZ//B3PW91/cc-pVTZ	0.00	0.26	2.39
CCSD(T)/cc-pVDZ//PBE1PBE/cc-pVTZ	0.00	0.28	2.32
CCSD(T)/cc-pVDZ//MP2/cc-pVDZ	0.00	0.39	2.45
CCSD(T)/cc-pVDZ//SCF/cc-pVDZ[a]	0.0	0.6	2.8
CCSD(T)/cc-pVDZ//LDA/plane wave[a]	0.0	0.0	1.7

[a]Reference 2.

comparison, the energy difference between the bowl and cage from the CCSD(T) calculations ranges from 0.26 to 0.39 eV. The latter results are in good agreement with those from multireference-MP2 calculations by Grimme and Muck-Lichtenfeld[16] and similar to those from CCSD(T)//SCF and CCSD(T)//LDA calculations by Taylor *et al.*[2] Although DFT (except PBE1PBE) calculations presented we yield inconsistent energy ordering with MP4 and CCSD(T), they (except TPSSKCIS) appear to give more reasonable HOMO-LUMO gaps (see Table IV). In contrast, the molecular-orbital calculations seem giving too large HOMO-LUMO gaps. Nevertheless, all calculations indicate that bowl has the largest HOMO-LUMO gap and is perhaps the most stable isomeric structure with high chemical stability.

On the other hand, many experiments[18–22] have demonstrated that ring should be the most stable C_{20} isomers at high temperature. Undoubtedly, to compare with experiments, thermochemical impacts should be considered to examine the relative stability of the three competitive C_{20} isomers.[59] We therefore undertook thermochemical analysis of the three neutral and anionic C_{20} isomers at the temperature from 0.5 to 3000 K. Calculations were based on the following equations:

$$\text{Sum of electronic energy and Gibbs free-energy correction} = E_0 + G_{\text{corr}}, \tag{1}$$

$$G_{\text{corr}} = H_{\text{corr}} - TS_{\text{tot}}, \tag{2}$$

$$H_{\text{corr}} = E_{\text{tot}} + k_B T, \tag{3}$$

$$E_{\text{tot}} = E_t + E_r + E_v + E_e, \tag{4}$$

$$S_{\text{tot}} = S_t + S_r + S_v + S_e, \tag{5}$$

where E_0 is the total electronic energy at $T=0$ K, G_{corr} and H_{corr} represent the thermal correction to Gibbs free energy and enthalpy, respectively. The internal thermal energy E_{tot} is contributed from translational (E_t), rotational (E_r), vibrational (E_v), and electronic (E_e) energies, and S_{tot}, S_t, S_r, S_v, S_e are the corresponding entropies. Figure 2 shows the relative total energies with Gibbs free-energy correction calculated at the PBE1PBE/cc-pVTZ level as a function of temperature. The relative stability of three neutral C_{20} isomers follows the ordering of bowl-cage-ring with bowl being the lowest-energy structure until the temperature is above 500 K, beyond which the ordering becomes ring-bowl-cage. This change in stability predicted from Gaussian thermochemical

TABLE IV. Energy gap (eV) between LUMO and HOMO for neutral C_{20} isomers.

Method	Bowl	Cage	Ring
B3LYP/cc-pVTZ	3.72	1.93	2.07
B3PW91/cc-pVTZ	3.74	1.95	2.04
PBE1PBE/cc-pVTZ	4.13	2.23	2.35
TPSSKCIS/cc-pVTZ	2.30	0.79	0.83
MP2/cc-pVDZ	9.13	6.38	6.52
MP4(SDQ)/cc-pVTZ//MP2/cc-pVDZ	9.10	6.32	···
CCSD(T)/cc-pVDZ//B3PW91/cc-pVTZ	9.58	6.67	7.19
CCSD(T)/cc-pVDZ//PBE1PBE//cc-pVTZ	9.59	6.68	7.22
CCSD(T)/cc-pVDZ//MP2/cc-pVDZ	9.13	6.38	6.52

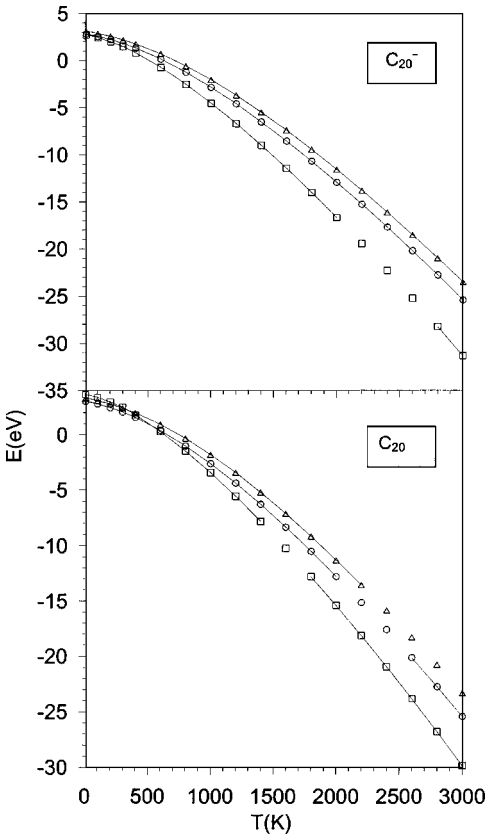

FIG. 2. Relative total energies with Gibbs free-energy corrections as a function of temperature. Thermochemical analysis were computed at the PBE1PBE/cc-pVTZ level. ○, bowl; △, cage; □, ring.

calculations[60] is different from that by Galli *et al.*[13] but in agreement with that by Brabec *et al.*[32]

For the three C_{20}^- anionic counterparts, we found again the energy ordering is quite sensitive to the hybrid functionals selected [see Tables V(A) and V(B)]. Both B3LYP and B3PW91 calculations yield the ordering of ring-bowl-cage with ring being the lowest in energy. In contrast, the PBE1PBE yields a bowl-ring-cage ordering, in which bowl and ring are nearly isoenergetic (with energy difference 0.09 eV) at $T=0$ K. On basis of the energy-ordering calculation for the neutral isomers, we speculated that the PBE1PBE functional is likely to give qualitatively correct energy ordering among the three C_{20}^- isomers. To confirm this speculation, we also performed single-point energy calculation at the MP4/cc-pVTZ level based on the geometries optimized at the PBE1PBE/cc-pVTZ level. As expected, the MP4 calculation suggests that the bowl is the lowest-energy structure of C_{20}^- isomers at $T=0$ K. Thus, the hybrid PBE1PBE method also shows good reliability in predicting the energy ordering among anionic low-lying isomers of C_{20}^-. On the other hand, thermochemical calculations based on PBE1PBE method yield the ring-bowl-cage ordering of C_{20}^- over the entire temperature range considered (Fig. 2), which is in agreement with that predicted by Lu *et al.*[15] According to this thermochemical analysis, ring is the most stable structure of C_{20}^- at high temperature, which agrees well with the experimental observations that ring is the dominant species in graphite vaporization sources at high temperature (~2000 K).[15]

TABLE VI. Calculated electron affinity (EA). All energies are in eV.

Method	Bowl	Cage	Ring
B3LYP/cc-pVTZ	2.26	2.23	2.92
B3PW91/cc-pVTZ	2.32	2.26	3.04
PBE1PBE/cc-pVTZ	2.23	2.26	2.96
Experiment[a]	2.25±0.03	2.17±0.03	2.44±0.03

[a]Reference 22.

C. Photoelectron spectra

PES have been reported for C_{20}^- clusters.[22] The spectra, however, are limited only up to 3 eV of binding energy. As such, the vibrational characterizations in the spectra have been used to distinguish the geometrical structures of three C_{20} isomers.[33] From the PES, the adiabatic detachment energy (ADE) can be measured, which is the energy needed to remove an electron from the anion to states of the neutral at their respective equilibrium geometries (denoted by R_A and R_N):[61]

$$\mathrm{ADE} = E_{\mathrm{tot}}(N,R_N) + Z_N - E_{\mathrm{tot}}(A,R_A) - Z_A, \tag{6}$$

where Z_N and Z_A represent zero-point energy correction to the neutral and anionic counterparts. The ADE obtained for the ground-state transition corresponds to the electron affinity (EA) of the neutral C_{20} isomers. Therefore, ADE is a measure of how tightly the cluster can bind an electron. Our calculated ADEs are compared with the experimental EAs

TABLE V. Calculated total energies (hartree) and relative energies (eV) for anionic C_{20}^- isomers.

Method	Bowl	Cage	Ring
(A)			
B3LYP/cc-pVTZ	−761.808 779 1	−761.740 399 4	**−761.870 067 9**
B3PW91/cc-pVTZ	−761.496 458 6	−761.470 721 6	**−761.515 738 0**
PBE1PBE/cc-pVTZ	**−760.913 791 9**	−760.909 929 5	−760.910 571 0
MP4(SDW)/cc-pVTZ//PBE1PBE/cc-pVTZ	**−759.896 469 8**	−759.865 406 3	−759.876 536 7
(B)			
B3LYP/cc-pVTZ	0.00	1.86	−1.67
B3PW91/cc-pVTZ	0.00	0.70	−0.52
PBE1PBE/cc-pVTZ	0.00	0.11	0.09
MP4(SDQ)/cc-pVTZ//PBE1PBE/cc-pVTZ	0.00	0.85	0.54

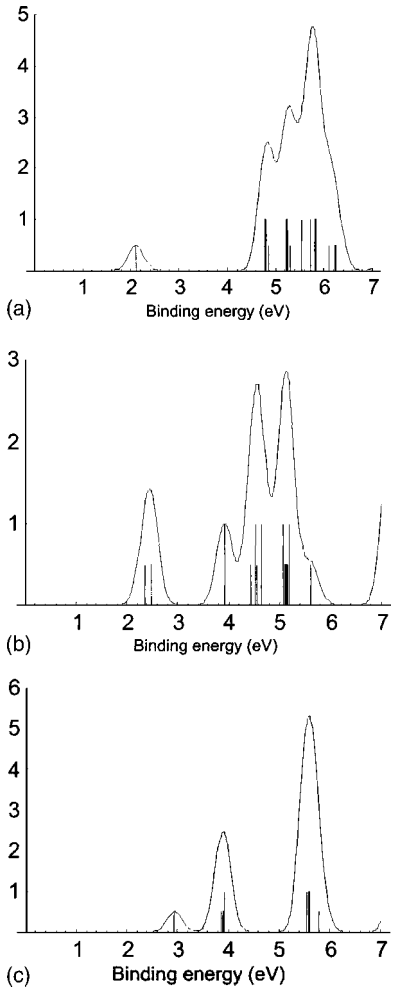

FIG. 3. Simulated photoelectron spectra for three C_{20}^- anionic isomers: (a) bowl, (b) cage, (c) ring. The spectra were constructed by fitting the distribution of the calculated energy eigenvalues with unit-area Gaussian functions of 0.05 eV full width at half maximum (FWHM). The values for VDEs calculation were obtained at the PBE1PBE/cc-pVTZ level.

(Ref. 22) in Table VI. All DFT values for bowl and cage show excellent agreement with the experimental values. For ring, however, the difference between the DFT calculations and the experimental is about 0.5 eV. Note that our calculations agree well with those by Lu *et al.*[15]

Vertical detachment energy (VDE) is the energy due to an instant detachment of an electron from an anion (A) to the corresponding neutral parent in some particular state N_l. VDE can be defined as

$$E_{b,i} = E_{\text{tot}}(N_i, R_A) - E_{\text{tot}}(A, R_A). \tag{7}$$

VDE contributes spectrally to a distinct peak from other PES characteristic peaks. Theoretically, PES can be evaluated by using the formula [Eq. (7)] given in Refs. 61 and 62. In order to derive more definitive features from theoretical calculations, we constructed the simulated PES up to 7 eV in binding energy. Figures 3(a)–3(c) display the characteristic peaks of PES for bowl, cage, and ring structures of C_{20}^-, respectively. It is evident that the energy gap between the first peak and main peaks for bowl is larger than that for cage and ring, which is consistent with the larger HOMO-LUMO gap of bowl compared to cage and ring[63] (see Table IV).

IV. CONCLUSIONS

We have performed high-level *ab initio* calculations to examine relative stability of three competitive isomers of C_{20} and C_{20}^-, respectively, and to simulate anion photoelectron spectra. Geometry optimizations have been performed using the three popular hybrid exchange-correlation functionals (i.e., B3LYP, B3PW91, PBE1PBE) and a new hybrid meta functional TPSSKCIS with a large cc-pVTZ basis set, respectively, as well as MP2 level with a moderate cc-pVDZ basis set. Single-point energies of the neutral isomers have been calculated at both the CCSD(T) level and the MP4 level to evaluate the energy difference among bowl, cage, and ring. The energy orderings given from DFTs show strong sensitivity to the hybrid functionals used. It is found that for the neutral isomers only the energy ordering given by PBE1PBE functional, i.e., the bowl-cage-ring ordering, is in qualitatively agreement with that given by CCSD(T) as well as MP4 calculations, irrespective of which theoretical method (DFT or MP2) is selected for geometrical optimization. Similarly, for the anionic counterparts, only the PBE1PBE calculation predicts the same energy ordering, i.e., the bowl-ring-cage ordering, as that predicted from MP4/cc-pVTZ calculation. The good reliability of the hybrid PBE method[64,65] in predicting the energy ordering for both neutral and anionic low-lying isomers of C_{20} and C_{20}^- suggests that this method should be a preferred choice when the DFT method is used in predicting relative stability among large-sized carbon clusters and nanostructures (e.g., finite-size nanotubes). To directly compare with the experiments, entropy effects must be considered. Our thermochemical calculations indicate that ring is the most stable structure for both neutral C_{20} and anionic C_{20}^- isomers at very high temperatures, in agreement with the experimental observations. This agreement suggests that the fullerene road may be a more likely way to fullerene formation. However, our calculations also show that bowl is likely the most stable structure of neutral C_{20} isomers at low to room temperatures (<500 K), suggesting the possibility of pentagon road to fullerene formation. Finally, we have computed photoelectron spectra of anionic C_{20}^- isomers. With binding energies up to 7 eV, the simulated PES show ample spectral features to distinguish the three competitive anionic C_{20}^- isomers. Hopefully, this simulation will stimulate further PES measurements in higher binding energy range of C_{20}^-.

ACKNOWLEDGMENTS

The authors thank Professor Lai-Sheng Wang and Nan Shao for valuable discussions. This research was supported in part by grants from U.S. Department of Energy (Grant No. DE-FG02-04ER46164), NSF (CHE, DMII, and MRSEC), John Simon Guggenheim Foundation and Nebraska Research Initiatives (X.C.Z.), and by the Research Computing Facility and Bioinformatics Facility at University of Nebraska-Lincoln.

[1] K. Raghavachari, D. L. Strout, G. K. Odom, G. E. Scuseria, J. A. Pople, B. G. Johnson, and P. M. W. Gill, Chem. Phys. Lett. **214**, 357 (1993).
[2] P. R. Taylor, E. Bylaska, J. H. Weare, and R. Kawai, Chem. Phys. Lett. **235**, 558 (1995).

[3]Z. Q. Wang, P. Day, and R. Pachter, Chem. Phys. Lett. **248**, 121 (1996).
[4]J. M. L. Martin, J. El-Yazal, and J.-P. Francois, Chem. Phys. Lett. **248**, 345 (1996).
[5]R. B. Murphy and R. A. Friesner, Chem. Phys. Lett. **288**, 403 (1998).
[6]E. Bylaska, P. R. Taylor, R. Kawai, and J. H. Weare, J. Phys. Chem. **100**, 6966 (1996).
[7]S. Sokolova, A. Lüchow, and J. B. Anderson, Chem. Phys. Lett. **323**, 229 (2000).
[8]L. Mitas, E. L. Shirley, and D. M. Ceperley, J. Chem. Phys. **95**, 3467 (1991).
[9]J. C. Grossman, L. Mitas, and K. Raghavachari, Phys. Rev. Lett. **75**, 3870 (1995).
[10]A. Castro, M. A. L. Marques, J. A. Alonso, G. F. Bertsch, K. Yabana, and A. Rubio, J. Phys. Chem. **116**, 930 (2002).
[11]A. H. Romero, D. Sebastiani, R. Ramirez, and M. Kiwi, J. Phys. Chem. **366**, 134 (2002).
[12]R. O. Jones and G. Seifert, J. Chem. Phys. **79**, 443 (1997).
[13]G. Galli, F. Gygi, and J.-C. Golaz, Phys. Rev. B **57**, 1860 (1998).
[14]M. Saito and Y. Miyamoto, Phys. Rev. Lett. **87**, 035503-1 (2001).
[15]J. Lu, S. Y. Re, Y.-k. Choe *et al.*, Phys. Rev. B **68**, 125415 (2003).
[16]S. Grimme and C. Muck-Lichtenfeld, ChemPhysChem **3**, 207 (2002).
[17]B. Paulus, Phys. Chem. Chem. Phys. **5**, 3364 (2003).
[18]G. von Helden, M.-T. Hsu, N. G. Gotts, P. R. Kemper, and M. T. Bowers, Chem. Phys. Lett. **204**, 15 (1993).
[19]Ph. Dugourd, R. R. Hudgins, J. M. Tenenbaum, and M. F. Jarrold, Phys. Rev. Lett. **80**, 4197 (1998).
[20]A. K. Ott, G. A. Rechtsteiner, C. Felix, O. Hampe, M. F. Jarrold, R. P. Van Duyne, and K. Raghavachari, J. Phys. Chem. **109**, 9652 (1998); W. Eberhardt, Phys. Rev. Lett. **74**, 1095 (1995).
[21]H. Handschuh, G. Ganteför, B. Kessler, P. S. Bechthold, and W. Eberhardt, Phys. Rev. Lett. **74**, 1095 (1995).
[22]H. Prinzbach, A. Weiler, P. Landenberger *et al.*, Nature (London) **407**, 60 (2000).
[23]H. W. Kroto, J. R. Heath, S. C. O'Brien, R. F. Curl, and R. E. Smalley, Nature (London) **318**, 162 (1985).
[24]K. Tanigaki, T. W. Ebbesen, S. Saito, J. Mizuki, J. S. Tsai, Y. Kubo, and S. Kuroshima, Nature (London) **352**, 222 (1991).
[25]Y. Achiba, T. Nakagawa, Y. Matusui *et al.*, Chem. Phys. Lett. **7**, 98 (1991).
[26]F. Henari, J. Callaghan, H. Stiel, W. Blau, and D. Cardin, Chem. Phys. Lett. **199**, 144 (1992).
[27]H. W. Kroto, Nature (London) **329**, 529 (1987).
[28]C. Piskoti, J. Yarger, and A. Zettl, Nature (London) **393**, 771 (1998).
[29]G. von Helden, N. G. Gotts, and M. T. Bowers, Nature (London) **363**, 60 (1993).
[30]A. Devos and M. Lannoo, Phys. Rev. B **58**, 8236 (1998).
[31]H. W. Kroto, K. Mckay, Nature (London) **331**, 328 (1988).
[32]C. J. Brabec, E. B. Anderson, B. N. Davidson, S. A. Kajihara, Q.-M. Zhang, and J. Bernholc, Phys. Rev. B **46**, 7326 (1992).
[33]M. F. Jarrold, Nature (London) **407**, 26 (2000).
[34]W. J. Hehre, L. Radom, P. von R. Schleyer, and J. A. Pople, *Ab Initio Molecular Orbital Theory* (Wiley, New York, 1986).
[35]W. Kohn and L. J. Sham, Phys. Rev. **140**, A1133 (1965).
[36]M. J. Frisch, G. W. Trucks, H. B. Schlegel *et al.*, GAUSSIAN 03, Revision B.03 ,Gaussian, Inc., Pittsburgh, PA, 2003.
[37]C. Lee, W. Yang, and R. G. Parr, Phys. Rev. B **37**, 785 (1988).
[38]A. D. Becke, J. Chem. Phys. **98**, 5648 (1993).
[39]J. P. Perdew, K. Burke, and Y. Wang, Phys. Rev. B **54**, 16533 (1996).
[40]K. Burke, J. P. Perdew, and Y. Wang, *Electronic Density Functional Theory: Recent Progress and New Directions* (Plenum, New York, 1998).
[41]J. P. Perdew, K. Burke, and M. Ernzerhof, Phys. Rev. Lett. **77**, 3865 (1996).
[42]J. P. Perdew, K. Burke, and M. Ernzerhof, Phys. Rev. Lett. **78**, 1396 (1997).
[43]Y. Zhao, B. J. Lynch, and D. G. Truhlar, Phys. Chem. Chem. Phys. **7**, 43 (2005).
[44]T. H. Dunning, Jr., J. Chem. Phys. **90**, 1007 (1989).
[45]C. Moller and M. S. Plesset, Phys. Rev. **46**, 618 (1934).
[46]M. Head-Gordon, J. A. Pople, and M. J. Frisch, Chem. Phys. Lett. **153**, 503 (1988).
[47]J. B. Foresman and A. Frisch, *Exploring Chemistry with Electronic Structure Methods*, 2nd ed. (Gaussian, Inc., Pittsburgh, PA, 1996).
[48]M. J. Frisch, M. Head-Gordon, and J. A. Pople, Chem. Phys. Lett. **166**, 281 (1990).
[49]M. Head-Gordon and T. Head-Gordon, Chem. Phys. Lett. **220**, 122 (1994).
[50]S. Saebo and J. Almlof, Chem. Phys. Lett. **154**, 83 (1989).
[51]J. A. Pople, R. Krishnan, H. B. Schlegel, and J. S. Binkley, Int. J. Quantum Chem. **14**, 545 (1978).
[52]K. Raghavachari, G. W. Trucks, M. Head-Gordon, and J. A. Pople, Chem. Phys. Lett. **157**, 479 (1989).
[53]K. Krishnan and J. A. Pople, Int. J. Quantum Chem. **14**, 91 (1978).
[54]G. W. Trucks, E. A. Salter, C. Sosa, and R. J. Bartlett, Chem. Phys. Lett. **147**, 359 (1988).
[55]G. W. Trucks, J. D. Watts, E. A. Salter, and J. Bartlett, Chem. Phys. Lett. **153**, 490 (1988).
[56]M. Saito and Y. Okamoto, Phys. Rev. B **60**, 8939 (1999).
[57]CERIUS^2, version3.8, Molecular Simulations Inc., San Diego, CA, 1998.
[58]GAUSSVIEW3.0, Gaussian, Inc., Pittsburgh, PA, 2002.
[59]K. M. Kadish and R. S. Ruoff, *Fullerenes_chemistry, Physics, and Technology* (Wiley-Interscience, New York, 2000), p. 300.
[60]http://www.gaussian.com/g_ur/k_freq.htm
[61]G. L. Gutsev, P. Jena, H. J. Zhai, and L. S. Wang, J. Chem. Phys. **115**, 7935 (2001).
[62]J. C. Rienstra-Kiracofe, G. S. Tschumper, and H. F. Schaefer III, Chem. Rev. (Washington, D.C.) **102**, 231 (2002).
[63]J. Li, X. Li, H. J. Zhai, and L. S. Wang, Science **299**, 864 (2003).
[64]M. Ernzerhof and G. E. Scuseria, J. Chem. Phys. **110**, 5029 (1999).
[65]C. Adamo and V. Barone, J. Chem. Phys. **110**, 6158 (1999).